

## Asymmetric Optical Second-Harmonic Generation from Chiral *G*-Shaped Gold Nanostructures

V. K. Valev,<sup>1,\*</sup> A. V. Silhanek,<sup>2</sup> N. Verellen,<sup>2,3,5</sup> W. Gillijns,<sup>2</sup> P. Van Dorpe,<sup>3</sup> O. A. Aktsipetrov,<sup>4</sup> G. A. E. Vandenbosch,<sup>5</sup>  
V. V. Moshchalkov,<sup>2</sup> and T. Verbiest<sup>1</sup>

<sup>1</sup>*Molecular Electronics and Photonics, INPAC, Katholieke Universiteit Leuven, Celestijnenlaan 200 D, B-3001 Leuven, Belgium*

<sup>2</sup>*Nanoscale Superconductivity and Magnetism & Pulsed Fields Group, INPAC, Katholieke Universiteit Leuven, Celestijnenlaan 200 D, B-3001 Leuven, Belgium*

<sup>3</sup>*IMEC, Kapeldreef 75, 3001 Leuven, Belgium*

<sup>4</sup>*Department of Physics, Moscow State University, 11992 Moscow, Russia*

<sup>5</sup>*ESAT-TELEMIC, K. U. Leuven, B-3001 Leuven, Belgium*

(Received 4 June 2009; published 26 March 2010)

We present a new electromagnetic phenomenon—the asymmetric second-harmonic generation from planar chiral structures. The effect consists in distinguishing the handedness of a chiral material by rotating the sample in an experiment involving solely linearly polarized light. This phenomenon originates in the surface plasmon resonance of chiral gold nanostructures, where homodyne interference of anisotropic and chiral electric and/or magnetic multipoles appears to play an important role.

DOI: 10.1103/PhysRevLett.104.127401

PACS numbers: 78.67.Bf, 42.65.Ky, 42.70.Qs

The remarkable expansion of nanoscience and nanotechnology during the past decade has led to strong interest in the investigation of nanoscale optical fields and the development of tools for their study. Consequently, the optical properties of metallic nanostructures are of great current significance from both fundamental and practical points of view [1]. One of the most important effects in light scattering by these nanostructures is the enhancement, up to several orders of magnitude, of the field intensity, which occurs in a confined nanoscale region around the particles. This enhancement originates from a combination of the electrostatic lightning-rod effect, due to the geometric singularity of sharp curvatures, and localized surface plasmon resonances. The latter are a consequence of the metal nanoparticle's ability to build up structural resonances of the collective oscillations of the metal electron plasma. The resonances depend on the particle's geometry and dielectric properties, as well as on the refractive index of its surroundings.

Second-harmonic generation (SHG) is known to be surface and interface sensitive on the atomic scale. Therefore, its application to the study of the nonlinear optical response of metal nanostructures, with their pronounced optical resonances and high surface-to-volume ratio, is particularly suitable for improving the insight into the relationship between optical properties and morphology at the nanoscale.

Symmetry issues are closely related to the polarization dependence of the nonlinear optical responses since, within the electric dipole approximation, SHG is forbidden in materials with inversion symmetry. Planar nanostructures are particularly interesting because, using modern lithography techniques, dielectric and metallic forms of complicated geometry can be created, including planar chiral designs [2,3]. The types of structures have recently

attracted a lot of interest as, for example, negative refractive index in chiral metamaterials was reported [4,5].

So far, all optical effects sensitive to chirality contained an electric dipole contribution.

In this Letter we report on a new optical phenomenon, in which the chirality of a patterned thin film is revealed by sample rotation—a unique and counterintuitive procedure, since chirality is normally invariant under rotation symmetry. This effect involves solely linearly polarized light. The film consisted of an arrangement of *G*-shaped gold nanostructures, as shown in the center of Fig. 1(a). Upon azimuthal sample rotation, the corresponding SHG response was found to be chiral; i.e., it shows the presence of asymmetries with a sense of rotation (lack of mirror symmetry). Furthermore, this sense of rotation reverses with the handedness configuration [*G* and mirror *G*, see Fig. 1(b)]. The effect originates in the surface plasmon resonance of the chiral gold nanostructures, where it appears that the simultaneous occurrence of different higher-order multipolar radiation mechanisms [6], i.e., magnetic dipoles and electric quadrupoles, play an important role. Contrary to previously reported optical effects sensitive to chirality, the asymmetric second harmonic generation (ASHG) presented in this Letter can occur without an electric dipole contribution.

SHG measurements were performed with a Mai-Tai femtosecond laser system at a wavelength of 800 nm. The samples consist of an array of nanostructures defined by electron-beam lithography, Au (25 nm) deposition, and standard lift-off procedure, see Fig. 1(b). For further details on the experimental setup and the sample preparation, see Ref. [7].

The second-harmonic response can be described by a nonlinear polarization, which is expressed in the electric dipole approximation as [8]:  $P_i^{\text{NL}}(2\omega) = \chi_{ijk}^{(2)} E_j(\omega) E_k(\omega)$ ,

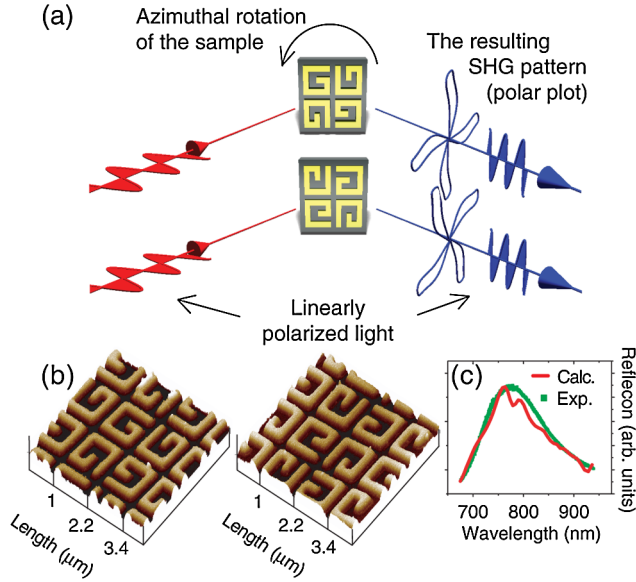


FIG. 1 (color online). (a) A schematic diagram illustrating the ASHG effect: upon azimuthal rotation of the sample, for linearly polarized light, the resulting SHG pattern exhibits a different sense of rotation and a different intensity depending on the handedness. (b) Atomic force microscope images of the two sample structures, *G* (left) and mirror-*G* (right). (c) Reflection spectra obtained experimentally and by means of a calculation.

where  $\omega$  is the frequency of light,  $\chi_{ijk}^{(2)}$  is the second order susceptibility tensor,  $E(\omega)$  the electric field component of the incident light, and  $i, j$ , and  $k$  are the Cartesian indices. It follows from this formula that SHG can only be generated in noncentrosymmetric materials or regions of matter that lack inversion symmetry, such as surfaces and interfaces. For an in-plane fourfold symmetric chiral sample the second order susceptibility that are different from zero are  $\chi_{zxx} = \chi_{zyy}$ ,  $\chi_{xxz} = \chi_{yyz}$ ,  $\chi_{zzz}$ , and  $\chi_{xyz} = -\chi_{yxz}$ . Often this last component is referred to as the “chiral” one, since it is present only in chiral systems. The other components are referred to as “achiral” because they occur in both chiral and achiral systems. By selecting the polarizer-analyzer combination, both the chiral and the achiral contributions can be probed separately. Furthermore, the presence of chiral and achiral components is not only limited to electric dipoles but also extends to the tensors of higher-order multipoles.

The total SHG intensity can be expressed as

$$I(2\omega) \propto |L(2\omega)\chi^{(2)}L^2(\omega)E(\omega)E(\omega)|^2, \quad (1)$$

where the terms  $L(\omega)$  and  $L(2\omega)$  designate the local field factors at the fundamental and at the second harmonic, respectively.

Because of the absorption in the bulk gold at the double frequency and to the geometry of the nanostructures, there is no local plasmon resonance at that wavelength and we can ignore the term  $L(2\omega)$ . Next, the symmetry of the local field factor  $L(\omega)$  is expected to be identical to that of the structures themselves and therefore to that of the suscep-

tibility  $\chi^{(2)}$ . We can therefore consider an effective four-fold symmetry for the susceptibility and the local field factors. This fourfold symmetric term can be described as  $\chi_{\text{eff}}^{(2)} \propto A[a^{\text{iso}} + \sin(4\theta)]$ , with  $a^{\text{iso}}$  being an isotropic term,  $A$  the amplitude, and  $\theta$  the angle of azimuthal rotation. Furthermore, the terms in  $\chi_{\text{eff}}^{(2)}$  contain both chiral and achiral contributions with different phase, which interfere in a homodyne manner, leading to  $|\chi_{\text{eff}}^{(2)}|^2 \propto A[\pm a^{\text{iso}} + \sin(4(\theta + \varphi))]^2 + B[b^{\text{iso}} + \sin(4(\theta + \phi))]^2$ , where the  $\pm$  sign indicates that the terms changes sign depending on the handedness of the structure,  $B$  and  $b^{\text{iso}}$  are again an amplitude and an isotropic term, and  $\varphi$  and  $\phi$  are phase terms. Finally, because of the complex geometry of the structures, there can be several pairs of these chiral and achiral contributions.

Figure 2(a) shows the SHG intensity as a function of the azimuthal rotation angle of the sample for both the *G* and the mirror-*G* structures, with the polarizer along the horizontal and the analyzer along the vertical direction (i.e.,  $P_{\text{IN}}-S_{\text{OUT}}$ ). This polarizer-analyzer combination addresses directly the chiral tensor element  $\chi_{yxz}$  and is therefore

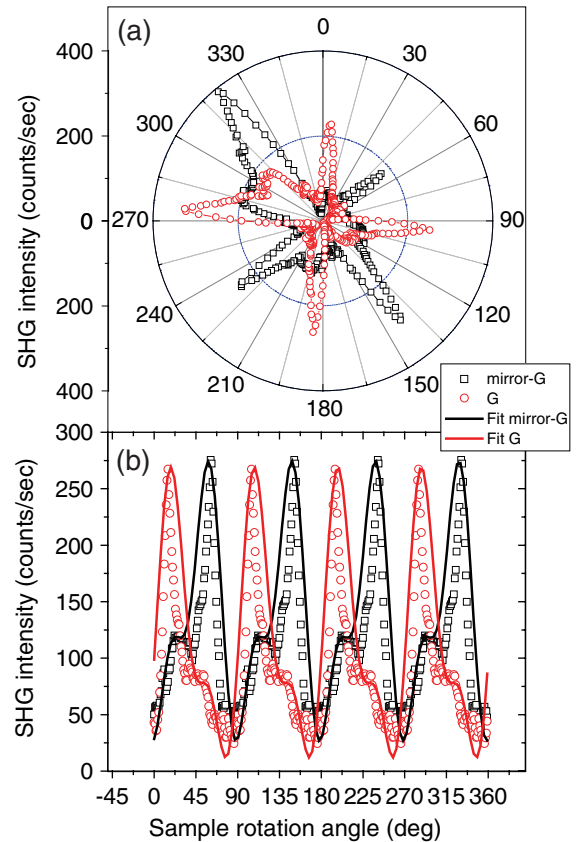


FIG. 2 (color online). The SHG intensity as a function of the azimuthal rotation angle of the sample for both chiralities. The polarizer was oriented along the horizontal direction while the analyzer was positioned along the vertical direction. In (a), the raw data from the experiment. In (b), the effective averaged response and the simulation of the SHG intensities for both chiralities.

highly sensitive to chirality in the samples. Indeed, Fig. 2(a) shows a dramatic dependence of the SHG response on the handedness. Both samples exhibit a fourfold pattern, with a  $45^\circ$  phase shift between the two, resulting in a pronounced SHG intensity difference for most sample orientations. Please note that in this experiment the laser spot is not *exactly* positioned on the center of rotation for practical reasons. In other words, while the sample is rotating the laser spot moves along a small circle and illuminates regions of the sample that can be slightly different in terms of thickness of the Gs and/or sharpness of their corners. These small variations in sample structure are due to the lift-off process and they are the reason why the amplitude of the four peaks in Fig. 2(a) can differ. Furthermore, the fourfold star is asymmetric itself; i.e., it presents a sense of rotation (lack of mirror symmetry), which also reverses with the handedness. It should be noted that in the  $P_{IN}-S_{OUT}$  configuration, the large chiral contribution from  $\chi_{yxz}$  is electric dipole allowed and that it is very likely dominating the signal.

Figure 3(a), however, shows the SHG intensity as a function of the azimuthal rotation angle of the sample for both chiralities, with both the polarizer and the analyzer

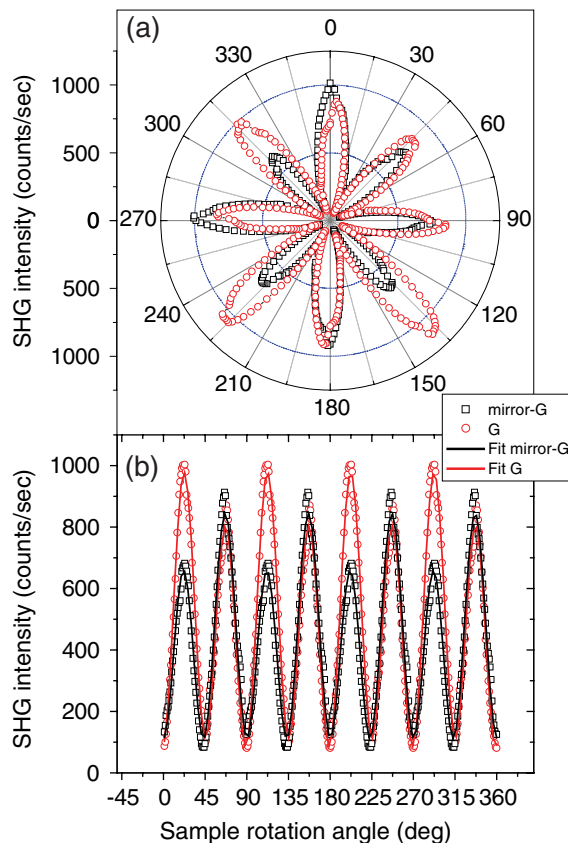


FIG. 3 (color online). The SHG intensity as a function of the azimuthal rotation angle of the sample for both chiralities. Both the polarizer and the analyzer were set along the vertical direction. In (a), the raw data from the experiment. In (b), the effective averaged response and the simulation of the SHG intensities for both chiralities.

along the vertical direction (i.e.,  $S_{IN}-S_{OUT}$ ). In this particular polarizer-analyzer configuration electric dipole contributions are forbidden, since  $\chi_{yyy} = 0$ . Consequently, the SHG response in Fig. 3(a) can be attributed to higher-order multipoles only, which could be associated either with the “bulk” of the material (regions other than the interfaces) or with its surface plasmon resonance. However, the amplitude of this multipole-induced signal is much too large for a bulk response from either the gold or the substrate and can therefore only be originating from the surface plasmon resonance field enhancement of the nanostructures. Indeed, Figs. 4(a) and 4(b) show the SHG signal from the substrate in the  $P_{IN}-S_{OUT}$  and the  $S_{IN}-S_{OUT}$  polarizer-analyzer configurations, respectively. The data show that the total amplitude of the substrate does not exceed 10 counts/sec and demonstrate the excellent signal-to-noise ratio of the setup. The presence of such a resonance near 800 nm was experimentally and theoretically verified [see Fig. 1(c) and Ref. [7]]. Clearly, the intensity of the peaks in Fig. 3(a) is affected by chirality and therefore the second-harmonic light is generated with different efficiency depending on the handedness of the sample. To our best knowledge, up to now, every optical effect sensitive to chirality contained electric dipole contributions. Henceforth, ASHG is the first electromagnetic phenomenon whereby chirality can be revealed through an interaction of higher-order multipoles only.

In order to investigate the origin of the ASHG effect, a phenomenological simulation of the second-harmonic signals was performed. The experimental data in both Figs. 2(a) and 3(a) indicate a fourfold anisotropy, which originates in the fourfold symmetry of the nanostructures’ unit cell. Consequently, the data points are several times redundant and could be averaged four times, thereby improving the signal-to-noise ratio of the relevant  $0^\circ$  to  $90^\circ$

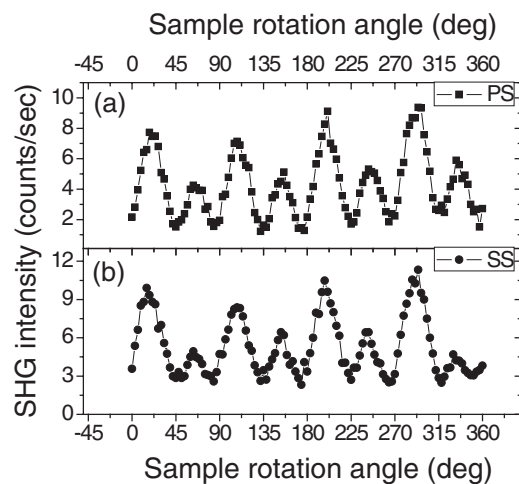


FIG. 4. The SHG intensity as a function of the azimuthal rotation angle of the sample substrate. In (a), the polarizer was oriented along the horizontal direction ( $P$ ) while the analyzer was positioned along the vertical direction ( $S$ ). In (b), both the polarizer and the analyzer were set along the vertical direction.

TABLE I. The values of the parameters that were used for simulating the SHG response in Figs. 2(b) and 3(b) with Eq. (2).

	$a_1$	$b_1$	$a_2$	$b_2$	$\varphi_1$	$\phi_1$	$\varphi_2$	$\phi_2$	$A_1$	$B_1$	$A_2$	$B_2$	$bg$
<i>P-S mirror-G</i>	-0.4	1.2	-0.4	1.2	7	-12.8	7	-12.8	100.6	15	15	5	24
<i>P-S G</i>	0.4	1.2	0.4	1.2	7	-12.8	7	-12.8	91.3	13	20	5	11
<i>S-S mirror-G</i>	-0.07	0.05	0	0	44.3	-39	0	0	694	142	0	0	74
<i>S-S G</i>	0.07	0.05	0	0	44.3	-39	0	0	518	167	0	0	88

region. Subsequently, this average was reproduced four times to provide matching boundary conditions for the simulation, i.e., to avoid a divergence beyond 90°. These averaged data points are shown as open symbols in Figs. 2(b) and 3(b).

The simulation curves in Fig. 2(b) were obtained with Eq. (1), where two pairs of interfering chiral and achiral contributions were considered in the effective susceptibility:

$$|\chi_{\text{eff}}^{(2)}|^2 \propto \sum_{i=1}^2 A_i [\pm a_i^{\text{iso}} + \sin 4(\theta + \varphi_i)]^2 + B_i [b_i^{\text{iso}} + \sin 4(\theta + \phi_i)]^2, \quad (2)$$

where the index  $i$  designates the pair number. It should be noted that for the simulations, all achiral terms except the amplitudes were identical for both *G* and mirror-*G* curves and only  $a_i^{\text{iso}}$  was considered to be chiral, i.e., was allowed to change sign. The amplitudes were allowed to differ, since two physically separate samples were measured. Nevertheless, the values for the amplitude parameters that were obtained are very similar, see Table I.

With these restrictive constraints, as it can be seen in Fig. 2(b), the simulation curves reproduce well the essential features of the data, especially the asymmetric nature of the SHG patterns. Similarly, the simulations in Fig. 3(b) clearly follow the intensity dependence of the peaks.

The ASHG effect can be attributed to a combination of plasmonic excitations in the nanostructures and lightning-rod effect enhancements of the electromagnetic fields. These were clearly shown to occur in our structures by SHG microscopy and it was demonstrated that they exhibit very unusual nonlinear optical properties. The fact that ASHG occurs also without electric dipole contributions can be explained by the fact that in the regions of large electromagnetic field enhancement, higher-order multipoles can play an important role.

Physically, two sorts of multipoles can be distinguished: those originating in Mie's theory [9] as size and retardation effects and those associated with microscopic multipole moments in the light-matter Hamiltonian [10]. Despite some phenomenological approaches to the problem [11,12], a first-principle microscopic theory for the nonlinear properties of nanoscale structures, providing a framework for the complete understanding of the new nonlinear optical effect presented here, is still lacking. Nevertheless, it should be noted that, recently, significant progress has been achieved in relating classical optical

calculations to SHG properties [13]. Our work clearly motivates further intense research in this area.

In conclusion, we presented on a new electromagnetic phenomenon, which is characterized by a sense of rotation in the second-harmonic intensity pattern, recorded upon azimuthal sample rotation. This sense of rotation reversed with the handedness of the structures. The effect originates in the surface plasmon resonance of the chiral gold nanostructures. In contrast to previous optical phenomena in chiral systems, which all contained an electric dipole contribution, the effect reported in this Letter was also observed in an interference between higher-order multipoles only.

We acknowledge financial support from the Fund for scientific research Flanders (FWO-V), the University of Leuven (GOA), Methusalem Funding by the Flemish government, and the Belgian Inter-University Attraction Poles IAP Programmes. V. K. V., A. V. S., P. V. D., and W. G. are grateful for the support from the FWO-Vlaanderen. O. A. A. is partly supported by the Russian Foundation for Basic Research.

\*Corresponding author.

v.k.valev@fys.kuleuven.be

www.valev.org

- [1] L. Novotny and B. Hecht, *Principles of Nano-Optics* (Cambridge University Press, Cambridge, 2006).
- [2] A. Papakostas *et al.*, Phys. Rev. Lett. **90**, 107404 (2003).
- [3] A. S. Schwanecke *et al.*, Phys. Rev. Lett. **91**, 247404 (2003).
- [4] S. Zhang *et al.*, Phys. Rev. Lett. **102**, 023901 (2009).
- [5] E. Plum *et al.*, Phys. Rev. B **79**, 035407 (2009).
- [6] O. A. Aktsipetrov *et al.*, J. Opt. Soc. Am. B **22**, 138 (2005).
- [7] V. K. Valev *et al.*, Nano Lett. **9**, 3945 (2009).
- [8] T. Verbiest, K. Clays, and V. Rodriguez, *Second-Order Nonlinear Optical Characterization Techniques* (CRC Press, New York, 2009).
- [9] W. S. Fan *et al.*, Opt. Express **14**, 9570 (2006).
- [10] R. Loudon, *The Quantum Theory of Light* (Oxford University Press, New York, 1983), 2nd ed.
- [11] K. Li, M. I. Stockman, and D. J. Bergman, Phys. Rev. Lett. **91**, 227402 (2003).
- [12] J. I. Dadap, J. Shan, K. B. Eisenthal, and T. F. Heinz, Phys. Rev. Lett. **83**, 4045 (1999).
- [13] Y. Zeng, W. Hoyer, J. Liu, S. W. Koch, and J. V. Moloney, Phys. Rev. B **79**, 235109 (2009).